Title: 3D Printing of Tablets Using Inkjet with UV Photoinitiation

Authors: Elizabeth A. Clark, Morgan R. Alexander, Derek J. Irvine, Clive J. Roberts, Martin J. Wallace, Sonja Sharpe, Jae Yoo, Richard J.M. Hague, Chris J. Tuck, Ricky D. Wildman

PII: S0378-5173(17)30593-8
DOI: http://dx.doi.org/doi:10.1016/j.ijpharm.2017.06.085
Reference: IJP 16809

To appear in: *International Journal of Pharmaceutics*

Received date: 3-5-2017
Revised date: 25-6-2017
Accepted date: 28-6-2017

Please cite this article as: Clark, Elizabeth A., Alexander, Morgan R., Irvine, Derek J., Roberts, Clive J., Wallace, Martin J., Sharpe, Sonja, Yoo, Jae, Hague, Richard J.M., Tuck, Chris J., Wildman, Ricky D., 3D Printing of Tablets Using Inkjet with UV Photoinitiation.International Journal of Pharmaceutics http://dx.doi.org/10.1016/j.ijpharm.2017.06.085

3D Printing of Tablets Using Inkjet with UV Photoinitiation

Elizabeth A. Clark[a], *Morgan R. Alexander*[b], *Derek J. Irvine*[a], *Clive J. Roberts*[b], *Martin J. Wallace*[c], *Sonja Sharpe*[d], *Jae Yoo*[d], *Richard J.M. Hague*[a], *Chris J. Tuck*[a], *Ricky D. Wildman*[a*]

[a] Faculty of Engineering, The University of Nottingham, University Park, Nottingham, NG7 2RD, UK
[b] Advanced Materials and Healthcare Technologies, School of Pharmacy, The University of Nottingham, University Park, Nottingham, NG7 2RD, UK

[c] Advanced Manufacturing Technology, GlaxoSmithKline (Ireland), 12 Riverwalk, Citywest, Business Campus, Dublin, 24, Ireland

[d] Advanced Manufacturing Technology, GlaxoSmithKline, 709 Swedeland Rd., UW2108, King of Prussia, PA 19406-0939, USA

[*] Corresponding author
E-mail: Ricky.Wildman@nottingham.ac.uk
Telephone: + 44 (0) 115 951 5559
Faculty of Engineering, University of Nottingham, University Park, Nottingham, NG7 2RD, UK

Graphical Abstract

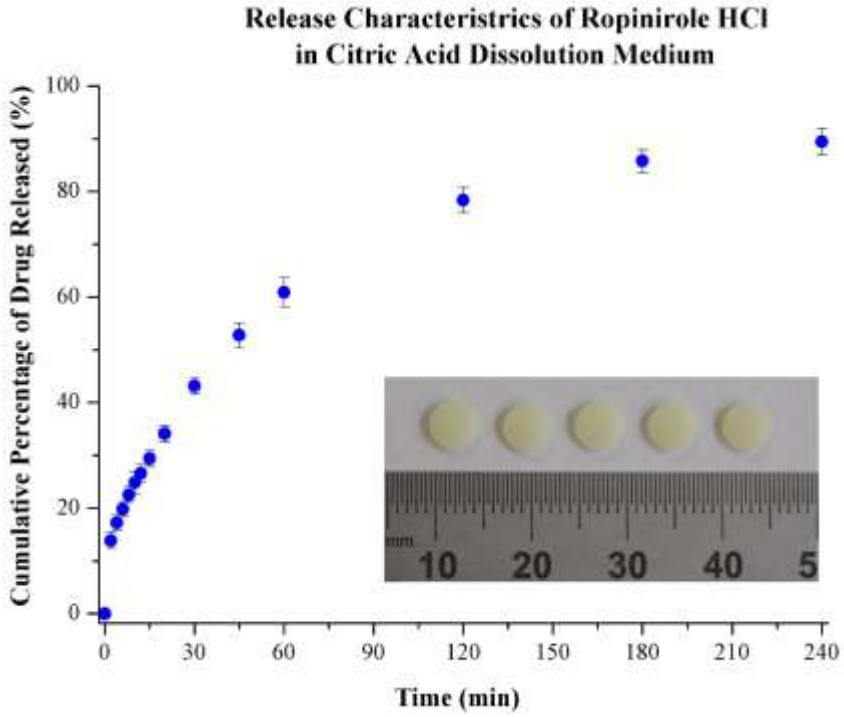

Abstract

Additive manufacturing (AM) offers significant potential benefits in the field of drug delivery and pharmaceutical/medical device manufacture. Of AM processes, 3D inkjet printing enables precise deposition of a formulation, whilst offering the potential for significant scale up or scale out as a manufacturing platform. This work hypothesizes that suitable solvent based ink formulations can be developed that allow the production of solid dosage forms that meet the standards required for pharmaceutical tablets, whilst offering a platform for flexible and personalised manufacture. We demonstrate this using piezo-activated inkjetting to 3D print ropinirole hydrochloride. The tablets produced consist of a cross-linked poly(ethylene glycol diacrylate) (PEGDA) hydrogel matrix containing the drug, photoinitiated in a low oxygen environment using an aqueous solution of Irgacure 2959. At a Ropinirole HCl loading of 0.41mg, drug release from the tablet is shown to be Fickian. Raman and IR spectroscopy indicate a high degree of cross-linking and formation of an amorphous solid dispersion. This is the first publication of a UV inkjet 3D printed tablet. Consequently, this work opens the possibility for the translation of scalable, high precision and bespoke ink-jet based additive manufacturing to the pharmaceutical sector.

Keywords

drug delivery, tablet, additive manufacturing, inkjet 3D printing, UV photopolymerization

Chemical compounds studied in this article

Ropinirole HCl (PubChem CID: 68727); Poly(ethylene glycol) diacrylate (PubChem CID: 16212859)

1. Introduction

With the Federal Drug Administration's (FDA) approval (FDA, 2015) of Spritam (the first commercially produced 3D printed medication, Aprecia Pharmaceuticals) there has been a

further increase in interest in additive manufacturing (AM) based platforms to produce both personalized medicines and novel function (Alomari et al., 2015). Inkjet printing has been highlighted as a promising additive method due to its precision, accuracy, low cost, ability to deposit multiple materials contemporaneously, and simple scale up/out, with material throughput being dependant on the size of the printer and number of jets (Alomari et al., 2015; de Gans et al., 2004; Daly et al. 2015). It is a well-established tool for commercial and consumer image production, and has been incorporated into 3D printing methods for prototyping (O'Neil, 2012) and manufacture (FDA, 2015). For example, the manufacture of Spritam uses a binder jetting method whereby an aqueous binder solution is jetted onto a powder-bed (O'Neil, 2012; Rowe et al., 2000) in order to build high dose, porous 3D tablet structures which can rapidly disintegrate (FDA, 2015). Recent reports of inkjet printed medicines have been focused mainly on polymer melts and solutions, which are solidified by drying or cooling and require carrier substrates. Hence, the potential to rapidly produce free standing solid dosage forms using UV curable materials has yet to be explored in inkjet printing.

Drop on demand (DoD) printing is a non-contact print method which employs either piezoelectric or thermal mechanisms to eject a droplet from the printhead nozzle. In either method, a series of droplets are precisely deposited onto a substrate in order to produce two-dimensional images. Three-dimensional (3D) objects can be generated by sequentially printing / depositing successive two-dimensional (2D) images over multiple layers. However, materials availability for inkjet printing are limited, and efforts to broaden the materials range for biotechnology applications is an active area of AM research (Begines et al., 2016; He et al., 2016; Hart et al. 2016; Saunders and Derby, 2014; Gudapati et al., 2016). In addition to inkjet 3D printing, other 3D printing technologies have shown significant progress (Alhnan et al., 2016; Goyanes et al., 2015; Khaled et al., 2015a, 2015b; Okwuosa et al., 2016; Sadia et al., 2016). Paste based extrusion printing (Khaled et al., 2015a, 2015b) and fused deposition

modelling (Goyanes et al., 2015; Okwuosa et al., 2016; Sadia et al., 2016) have demonstrated the potential of fabricating immediate and extended release dosage forms, as well as printing "polypills" which contain multiple actives (Goyanes et al., 2015; Khaled et al., 2015a, 2015b), starting from approved pharmaceutical grade excipients.

Recent research in inkjet printed pharmaceuticals has focused on solutions (Alomari et al., 2015; Genina et al., 2013; Scoutaris et al., 2011; Sandler et al., 2011; Raijada et al., 2013; Lee et al., 2012; Acosta-Vélez et al. 2017), nanosuspensions (Pardeike et al., 2011), and melts (Içten et al., 2015; Zhu et al., 2013), each of which is primarily 2D. Reel to reel type flexographic (Raijada et al., 2013; Palo et al., 2015) printing, as well as inkjet printing in combination with electrospinning (Palo et al., 2017) have also been utilized. Sandler *et al.* investigated the release profiles and crystallization behaviour of inkjet-printed solutions of paracetamol, theophylline, and caffeine on edible films and porous paper (Sandler et al., 2011). Varan *et al.* has investigated the prolonged release behaviour of inkjet printed paxitaxel in a cyclodextrin inclusion complex and cidofovir encapsulated in polycaprolactone nanoparticles dispensed onto bioadhesive films (Varan et al., 2017). Low melting temperature PEG/naproxen mixtures (Içten et al., 2015; Zhu et al., 2013; Hsu et al., 2015) have been reported for melt based inkjet applications in which crystalline domains of the drug could be affected by PEG coatings (Hsu et al., 2015), or controlled melt cooling (Içten et al., 2015). Lee *et al.* successfully produced paxlitaxel loaded poly(lactic-*co*-glycolic acid) microparticles with various geometries (honeycombs, grids, rings and circles) and observed that the drug release rate was dependant on the surface area of the microparticles (Lee et al., 2012). However, these printing methods are limited in that the doses produced are films, often with an edible substrate incorporated into the dosage form. Evaporation of solvent, or cooling of the melt is also necessary in order to solidify the dose. A recent development is that of Acosta-Vélez *et al*. who reported a biocompatible and photocurable ropinirole HCl loaded ink which can be piezo printed, but

requires a multistep process involving the manufacture of preformed ‘tablets’ into which the ink is deposited (Acosta-Vélez et al., 2017).

UV curing is widely used in the inkjet printing industry (Yeates et al., 2012) to rapidly solidify materials on demand. In this process the ink contains cross-linkable functional groups designed to be triggered by light, often with a photoinitiator promoting the process (Yeates et al., 2012). Similarly, photocross-linkable resins are used in stereolithography (SLA) printing, an AM process in which a vat of the resin is precisely cured by a laser in a layer by layer process to generate a 3D object. The suitability and mechanical properties of drug loaded UV curable inks have recently been evaluated for SLA based systems (Vehse et al., 2014; Wang et al., 2016) with major advantages being the capability to build scaffolds and complex (torus) tablet geometries with extended release profiles at ambient temperature (Wang et al., 2016). Despite the advantages, however, UV curable inkjet printable formulations have not been reported for the fabrication of solid dosage forms. Being able to combine 3D inkjet based printing with UV curing offers high resolution, rapid curing and the ability to alter geometry and material composition in a flexible, tuneable way. Furthermore, scale-up/out and speed-up of the process for commercial production has the potential to be achieved via increasing the number of jetting nozzles and/or printheads.

The scarcity of available photopolymerizable materials and high efficiency photoinitiators which are either generally regarded as safe (GRAS) or FDA approved makes UV ink formulation challenging. PEG is recognized by the FDA as an inactive tablet ingredient (Maximilien, 2009). PEG diacrylate is a network forming free radical addition type cross-linker that exhibits biocompatibility (Hoffman, 2002). However, residual unreacted monomer and macromer (Norman et al., 2017), as well as photoinitiator related decomposition products may be of concern in solid dosage forms depending on the concentrations released during dissolution (Williams et al., 2005; Xu et al., 2015). Ropinirole HCl (REQUIP ®

GlaxoSmithKline Inc.), a dopamine agonist drug used in the treatment of Parkinson's and restless les syndrome, was chosen as an example drug in this study due to the range of oral doses commercially available. It is produced in immediate and extended release dosage forms ranging from 0.25 mg to 8.0 mg (GSK, 2015).

2. Materials and Methods:

2.1. Ink formulation

Inks were prepared with 0.50 wt % Irgacure 2959 photoinitator (BASF), 30 w t%, 2.00 wt % ropinirole HCl (Sequoia Research Products, >98%) and poly(ethylene glycol) diacrylate (PEGDA) (M= 700g mol^{-1}, Sigma Aldrich), Irgacure 2959 was stirred into the PEGDA at elevated temperature (110°C, 600 rpm) until dissolved. Water and the drug were then stirred into the solution (40°C, 600 rpm) until dissolved. The ink was then degassed with nitrogen for 10 minutes and filtered the solution through a 0.45 mm pore size hydrophilic 13mm diameter Millex PTFE filter (Sigma Aldrich) prior to cartridge loading. To block ambient light, which can prematurely cure the resin during ink formulation and printing, the ink vessel and cartridge were wrapped several times in silver duct tape. To minimize solvent loss during heating and degassing stages, the solution was sealed with a rubber septa cap. Base ink (i.e. API free) formulations, were prepared for control purposes and formulated with 2 wt % additional PEGDA in order to keep the water content constant. All materials were used as received.

2.2. Dynamic viscosity

In formulating the inks, the viscosity was measured and optimized using a Malvern Kinexus Rheometer (Worcester, UK) equipped with a cup and bob type sample geometry at (50°C) at fixed shear rate (100 s^{-1}). All measurements were performed in triplicate.

2.3. Surface tension

The surface tension was determined with a Kruss DSA Drop shape analyser at 23°C using the Pendant Drop Method. Ten drops were analysed for each ink.

2.4. Printing and processing parameters

The formulations were printed onto a poly(ethylene terephthalate) (PET) film substrate using a Dimatix Materials Printer (DMP-2830 Fujifilm, Lebanon, NH, USA). The printer was enclosed in a custom-built glove box and purged with nitrogen gas. O_2 levels were kept below 0.2 % (2000 parts per million, ppm) throughout processing to reduce and control oxygen concentrations which can inhibit the curing transformations (i.e. initiation and propagation). The Dimatix Materials Cartridge (DMC-11610, Fujifilm Dimatix) contains 16 linearly aligned jets, spaced 254 μm apart with a ~10 pL drop volume. Curing of the material was carried out during printing with a LED UV lamp (365nm, 600 mW cm^{-2}, Printed Electronics Limited, Tamworth, UK) bolted directly to the printhead mount and in-line with the print path at print cartridge height. He et al. have previously described this method to print polycaprolactone dimethacylate based inks (He et al., 2016). This curing unit follows the print and irradiates the deposited material during each print pass and at the same print speed. Jetting voltages for each nozzle ranged from 20.4 V to 22 V and were individually adjusted to achieve a uniform drop speed (1.000 mm per 0.128 ms) at 50°C. The image pattern was a 5.04 mm diameter circle bitmap with 847 dpi resolution, corresponding to a 30 mm drop spacing. An array consisting of twenty five tablets with a 10 mm (horizontal) start distance from one pattern to the next was then generated with the Dimatix Pattern Editor Software. The height of the cartridge was set to 1.00 mm for the first 100 layers, then repositioned to 1.25 mm for an additional 15 layers to provide adequate spacing between the tablet and cartridge as the tablet height increases. To post-cure the printed layers, the UV light was scanned over the samples at print speed a total

of ten times. To maximize printing speed, all nozzles (16 total) were used, using a high jetting-frequency (6 kHz) alongside the maximum power level on the UV LED power supply being activated. The total printing time was ~ 1.5 hours for each batch of 25 tablets (equating to ~4 minutes per tablet). To post-cure the printed layers, the UV LED light was scanned over the samples at print speed and final cartridge height (1.25 mm) a total of ten times. The post curing time was therefore ~7.5 minutes for each batch of 25 tablets (equating to ~18 s per tablet). To remove residual water, the prints were dried in a convection oven (Lenton, Eurotherm 3216 Controller) at 40°C overnight, and then removed from the substrate and stored in a vacuum desiccator.

2.5. Tablet swelling and leaching

Swelling of the tablets was carried out over nine days in 10mL deionized water media at 37°C. Media was replaced periodically (five times in total). Samples were carefully blotted with a lint free wipe and immediately weighed. Nine base ink tablets and five API tablets were analysed.

2.6. Dissolution testing, tablet assay and HPLC methods

The United States Pharmacopeia (USP) dissolution test II (USP, 2014) was implemented to characterize ropinirole HCl release. A 2.1g L^{-1} (0.011M) citric acid (99%, Sigma Aldrich) dissolution media was prepared with ultrapure 18.2MW-cm water, adjusted to pH=4.0 +/-0.1 with tris (hydroxymethyl) methylamine (99.9%, Sigma Aldrich), and degassed with He (g). Dissolution testing was carried out with a USP grade Erweka (Heusenstamm, Germany) DT600 series rig in five individual vessels, each containing 500mL +/- 0.01 mL of dissolution media and one printed dosage. The vessels were equilibrated to 37.0+/- 0.1°C and equipped with rotating USP type I baskets, rotated at 50 rpm. Samples of 5.0 mL were then extracted at times:

2, 4, 6, 8, 10, 12, 15, 20, 30, 45, 60, 120, 180, 240 minutes and filtered through 0.45 um pore size Millex hydrophilic PTFE membrane filters. To maintain constant vessel volume, 5.0 mL of dissolution media was added to each vessel after each extraction. The procedure was repeated for the five additional tablets. A standard calibration curve of ropinirole HCl in the dissolution medium was prepared to determine the API concentration in each sample and can be found in the **Supplementary Data** section (**Fig. S3**).

A Hewlett Packard Agilent (Santa Clara, CA, USA) 1050 series HPLC system equipped with an auto sampler, quaternary pump, degasser, and multi-wavelength UV detector, set at 250 nm, was used to detect the API. A 4.6mm x 25cm Supelco Discovery C18 reverse phase column (Sigma Aldrich) with 5um particle sized L1 type packing was used to separate the components of the samples at ambient temperature, using a flow rate of 1.0 ml/min and a 200 μL sample injection volume. HPLC Mobile phases were prepared according to USP specifications (USP, 2014) for ropinirole HCl. Briefly, the mobile phase consisted of an ammonium acetate (98% Sigma Aldrich) buffer solution, acetonitrile (Fisher Chemical), and methanol (Fisher Chemical), in the volume ratio of 40:7:3 respectively. The buffer solution consisted of 3.85 g L^{-1} ammonium acetate in water, adjusted to pH=2.50 +/- 0.01 with phosphoric acid. All solvents used were HPLC gradient grade.

To assay the API loaded tablets, a 4 ppm ropinirole HCl standard solution standard was prepared in ammonium acetate buffer from a 100ppm stock solution. Each tablet was dissolved in 100 mL of ammonium acetate buffer solution and stirred for ~2.5 days at room temperature. The samples were filtered with 0.45 um pore size PTFE filters (Millex) and were analysed at 30°C according to the USP method for ropinirole HCl. Testing was carried out in duplicate.

To analyse the base ink tablets, five base ink tablets were pulverized with a mortar and pestle, 35 mg of material was added to a 10mL volumetric flask and diluted to volume with ammonium acetate buffer. The sample was sonicated for 30 min and dissolved overnight with stirring at

room temperature. The samples were filtered with 0.45 um pore size PTFE membrane filters and analysed with the HPLC using an injection volume of 20 μL. It should be noted that this procedure was also performed on five pulverized drug tablets. Results for the drug containing tablets indicated incomplete drug release (< 50%). However dissolution may be incomplete.

2.7. FTIR

A Frontier FT IR-ATR (Perkin Elmer, Waltham, MA, USA) was used to analyse the samples. Samples were scanned from 4000 cm^{-1} to 600 cm^{-1} every in steps of 0.5 cm^{-1}. Three scans were run for each spectrum with a resolution of 2 cm^{-1}.

2.8. Confocal Raman

The collection of confocal Raman single point spectra was carried out with a JobinYvon/Horiba Raman Spectrometer equipped with a 784 nm infrared laser, 600 nm^{-1} grating, and 50x objective microscope. Slit width was 300 μm and collection time was 10s. Scans were made in duplicate. Mapping of 50 μm x50 μm area was carried out overnight for a total area of 400 points using a step size of 2.5 μm.

3. Results and Discussion

3.1. Ink characterization

The formulation and drop requirements for DoD inkjet printing have been extensively studied (Daly et al., 2015; Yeates et al., 2012; Martin and Hutchings, 2012; Derby, 2010; Soltman and Subramanian, 2008). Optimising the physical properties of the ink, such as the viscosity and surface tension, is important for producing drops that can be ejected from the printer. Fujifilm, for example, recommends an operating viscosity range of 2 to 30 centipoise (cP), and a surface tension of 30 mN m^{-1} for their Dimatix Printers (Fujifilm, 2008). The base ink and API

containing ink viscosities were 13.58 +/- 0.02 cP and 14.01 +/- 0.03 cP, respectively. The surface tension of the base ink and API ink were 40.60 +/- 0.14 mN m^{-1} and 39.07 +/- 0.30 mN m^{-1}, respectively.

3.2. Physical characterization of the printed dosage forms

Images of the printed tablets can be found in **Fig. 1a and Fig. 1d**. The tablets were opaque and light yellow, in contrast to their light yellow translucent ink solution appearance. Base ink (drug free) tablets and ink solutions were translucent and colourless **(Fig. S4)**. Estimated drug loading was 0.41 mg calculated based on the solvent free ink composition components and the average tablet mass. The average diameters and mass of the dry tablets are also given (**Table 1),** which are well within USP tablet specifications (≤5% weight deviation) (USP, 2000). Optical microscopy images in **Fig. 1b and Fig. S1** indicate some small "banding" defects along the direction of printing, likely caused by rapid solidification of the ink after deposition (Castrejon-Pita et al., 2013). This can be adjusted by decreasing the UV intensity or print speed, for example. Small patches also appear on the print surface. Cross polarized optical microscopy (**Fig.1c, Fig. S1**) indicated that the material in the tablet is amorphous.

3.3 Characterization of API content and tablet swelling

Swelling and leaching of both the base ink and active pharmaceutical ingredient (API) loaded tablets was carried out in deionized water and is summarized in **Table 2.** All tablets remained intact throughout the test. The percentage of extractable material in the base ink tablets was 2.7%, indicating low sol content in the gel. The degree of swelling was 44%; while swelling in the API loaded tablets was slightly higher (48%). The assayed printed tablets contained 0.39 +/- 0.01 mg of API material. The percentage recovery, was 97% +/- 0.4% indicating either a small amount of degradation of the API or incomplete drug release from the tablets. Degradation

of Ropinirole HCl has been reported to occur under oxidative, UV, thermal, high humidity (Reddy et al., 2014) and hydrolytic (Parmar et al., 2009; Reddy et al., 2014) conditions. Exposure of the drug to UV light, free radicals, water, or heat during the printing process could all affect the drug stability in the formulation and tablets. Additional HPLC peaks, were also observed in both the printed API and base ink formulations **(Fig. 2a),** likely corresponding to the photoinitiator and its related decomposition products (McGilvray, 2010), which can absorb light at the drug detection wavelength. Characteristic chromatograms for the tablet samples and standards, as well as for the photoinitiator, are presented in **Fig. 2a and Fig. S2,** respectively.

3.4. Drug Dissolution

To characterize drug release from the printed dosage forms, ten tablets were randomly selected for dissolution testing. The resultant drug dissolution profile is shown in **Fig. 2b.** The tablets released 89% of the API over four hours, with around 60% being released within the first hour, a feature likely owing to the high solubility of the API salt in water and the tablet geometry. It was observed that the tablets remained intact throughout the test.

The mechanism of drug release in the hydrogels was best fitted with the Korsmeyer-Peppas model (**Table S1)**. The Korsmeyer-Peppas model can be used to determine drug release from polymeric matrix systems according to Eq. (1)**,** where the fraction of drug released, $\frac{M_t}{M_\infty}$, at time, *t*, is represented (Korsmeyer et al., 1983; Riger and Peppas, 1987; Dash et al., 2010) by

$$\frac{M_t}{M_\infty} = Kt^n \quad (1)$$

where the release exponent, *n*, defines the type of diffusional transport (i.e. Fickian or non-Fickian mass transfer) (Riger and Peppas, 1987), *K* is the kinetic rate constant, M_t is the

amount of drug released at time, *t*, and M_∞ is the total amount of drug in the dosage form. In this model the first 60% of release data is plotted as the natural log cumulative percentage released versus natural log time to determine the release coefficient, *n*, which is given by the gradient of this relationship. It has previously been shown by Ritger and Peppas for cylindrical shaped tablets that $n \leq 0.45$ indicates Fickian transport of the drug from the matrix (Riger and Peppas, 1987). The release exponent of 0.43 determined for the hydrogels in this study, therefore indicates that Fickian diffusion is the primary mechanism of API release.

3.5. FTIR

Fourier transform infrared spectroscopy-attenuated total reflection (FTIR-ATR, Perkin-Elmer) was used to confirm the presence of the API and to assess the degree of cure on the tablet surfaces. A spectrum of crystalline ropinirole HCl is shown in **Fig. 3a.** Ropinirole HCl was observed to have characteristic peaks at 3218 cm^{-1}, 3071 cm^{-1} (a secondary amide N-H-stretch), 2601 cm^{-1} (a tertiary amine salt N-H+ stretch), 1703 cm^{-1} (amide C=O stretch), as well as 1614 cm^{-1}, 1597 cm^{-1}, and 775 cm^{-1}. For comparison, the uncured PEGDA macromer spectra has been included; it contains characteristic acrylate peaks at 1722 cm^{-1} (C=O stretch), 1636 $cm^{-1}$and 1618 cm^{-1} (acrylate C=C stretches) and 810cm^{-1} (acrylate $=CH_2$ twist) (Lin-Vien et al., 1991). The top and bottom tablet surfaces were found to contain the API peaks at 3071 cm^{-1}, 2601 cm^{-1}, 1597 cm^{-1}, 1703 cm^{-1} and 775 cm^{-1} confirming the presence of the drug. The acrylate related peaks at 810 cm^{-1}, and 1636 cm^{-1} were not present, indicating a high degree of acrylate functional group conversion.

3.6. Confocal Raman

Confocal Raman was then used to characterize the API in the top surface of the print. Single point spectra of the pure drug and the printed base ink, are shown in **Fig. 3b**. In the drug spectra,

a high intensity peak was observed in the fingerprint region at 480cm^{-1} as well as an amide (C=O stretch) at 1704cm^{-1}. In the cured based ink spectra, characteristic broad PEG-related peaks were observed, as well as a C=O stretch at 1731cm^{-1}. The spectra for the printed API ink formulations, which contain both the polymer matrix and photoinitiator is shown in **Fig. 3b**. Inspection of the spectra of the dosage form suggested that it was a combination of cross-linked base polymer and API with no evidence of API related peak broadening. The C=C acrylate stretching peak at 1636 cm^{-1} is also not observed in the single point spectra of the base ink or API loaded tablets, signalling high levels of cure. Therefore, only very low levels of unreacted di-acrylate monomer appear to remain in the material. Mapping of the API in the printed drug loaded tablets was carried out using the intensity of the drug related peak at 480 cm^{-1} (**Fig. 3c**). The drug related peak is detected throughout the entire mapped area, but variability of the intensity was noted. There appears to be at the micron scale drug poor regions as well as drug rich 'hot spots' in the tablet. To investigate this further, a distribution of the API (red) and base ink (blue) was determined by a Classical Least Squares Fit (**Fig. 3d**) to the mapped data using the pure API and cured base ink spectra as references. This fit is consistent with the API peak intensity mapping. Whilst there is evidence of heterogeneity in drug distribution at the micron scale none of these regions show evidence of drug crystallinity, strongly suggesting the formation of a solid dispersion. This is also consistent with the nature of the drug release observed for the API.

4. Conclusions

In summary, UV inkjet printing has been demonstrated as a platform to produce solid oral dosage forms for the first time. A novel UV curable, 3D printable ink was developed specifically for ropinirole HCl, a low dose water soluble drug. These tablets were characterized by Raman mapping, FTIR-ATR and optical microscopy and shown to be amorphous solid dispersions with high degrees of photopolymer curing. The drug release kinetics were

determined to follow the Korsmeyer-Peppas power law type release model with Fickian diffusion. It is anticipated that this approach can be used with a range of API and photoinitiator combinations, assuming compatibility and solubility of the components. As a consequence, solid dosage forms produced using this method will provide the opportunity for greater flexibility in the pharmaceutical industry in comparison to commonly adopted solid dosage manufacturing techniques in a variety of scenarios, including small scale clinical trials, personalized medicine, as well as functionally graded dosage design.

Acknowledgements
The work in this paper was funded by GlaxoSmithKline, Inc. and the Engineering and Physical Sciences Research Council under grant EP/I033335/2. Access to the Raman instrument was kindly provided by the Nottingham Nanoscale and Microscale Research Centre.

References

Acosta-Vélez et al. 2017 G.F. Acosta-Vélez, C.S. Linsley, M.C. Craig, B. M. Wu **Photocurable Bioink for the Inkjet 3D Pharming of Hydrophilic Drugs** Bioengineering, 4 (2017), pp. 11 doi:10.3390/bioengineering4010011

Alhnan et al., 2016 M.A. Alhnan, T.C. Okwuosa, M. Sadia, K.W. Wan, W. Ahmed, B. Arafat **Emergence of 3D Printed Dosage Forms: Opportunities and Challenges** Pharm. Res., 33 (2016), pp. 1817-1833. doi: 10.1016/j.jconrel.2011.07.033

Alomari et al., 2015 M. Alomari, F. H. Mohamed, A. W. Basit, S. Gaisford **Personalised dosing: Printing a dose of one's own medicine** Int. J. Pharm., 494 (2015), pp. 568-77 doi: 10.1016/j.ijpharm.2014.12.006

Begines et al., 2016 B. Begines, A.L. Hook, M.R. Alexander, C.J. Tuck, R.D. Wildman **Development, printability and post-curing studies of formulations of materials resistant to microbial attachment for use in inkjet based 3D printing** Rapid Prototyping J., 22 (2016), pp. 835-841 doi: 10.1108/RPJ-11-2015-0175

Castrejon-Pita et al., 2013 J.R. Castrejon-Pita, W.R.S. Baxter, J. Morgan, S. Temple, G.D. Martin, I.M. Hutchings **Future, opportunities and challenges of inkjet technologies** Atomization Spray., 23 (2013), pp. 541-565 doi: 10.1615/AtomizSpr.2013007653

Daly et al. 2015 R. Daly, T. S. Harrington, G. D. Martin, I.M. Hutchings **Inkjet printing for pharmaceutics - A review of research and manufacturing** Int. J. Pharm., 494 (2015), pp. 554-567 doi: 10.1016/j.ijpharm.2015.03.017

Dash et al., 2010 S. Dash, P.N. Murthy, L. Nath, P. Chowdry **Kinetic modeling on drug release from controlled drug delivery systems**, Acta Pol. Pharm., 67 (2010), pp. 217-223

de Gans et al., 2004 B-J. de Gans, P.C. Duineveld, U.S. Schubert **Inkjet Printing of Polymers: State of the Art and Future Developments** Adv. Mater., 16 (2004), pp. 203-213 doi: 10.1002/adma.200300385

Derby, 2010 B. Derby **Inkjet Printing of Functional and Structural Materials: Fluid Property Requirements, Feature Stability, and Resolution** Annu. Rev. Mater. Res., 40 (2010), pp. 395-414 doi: 10.1146/annurev-matsci-070909-104502

FDA, 2015 United States Food and Drug Administration, Highlights of Prescribing Information — Spritam, http://www.accessdata.fda.gov/drugsatfda_docs/label/2015/207958s000lbl.pdf, accessed: October, 2016.

Fujifilm, 2008 Fujifilm Dimatix, Materials Printer & Cartridge DMP-2800 Series Printer & DMC-11600 Series Cartridge. https://www.fujifilmusa.com/shared/bin/FAQs_DMP-2800_Series_Printer_DMC-11600+Series+Cartridge.pdf, 2008 (accessed 10.10.16)

Genina et al., 2013 N. Genina , E.M. Janßen, A. Breitenbach, J. Breitkreutz, N. Sandler **Evaluation of different substrates for inkjet printing of rasagiline mesylate** Eur. J. Pharm. Biopharm., 85 (2013), pp. 1075-1083 doi: 10.1016/j.ejpb.2013.03.017

Goyanes et al., 2015 A. Goyanes, J. Wang, A. Buanz, R. Martínez-Pacheco, R. Telford, S. Gaisford, A.W. Basit **3D Printing of Medicines: Engineering Novel Oral Devices with Unique Design and Drug Release Characteristics** Mol. Pharm., 12 (2015), pp. 4077-4084. doi: 10.1021/acs.molpharmaceut.5b00510

GSK, 2015 GlaxoSmithKline, Product Monograph REQUIP ® Ropinirole Hydrochloride Tablets. http://ca.gsk.com/media/592150/requip.pdf , 2015 (accessed 10.10.16)

Gudapati et al., 2016 H. Gudapati, M. Dey, I. Ozbolat **A Comprehensive Review on Droplet-based Bioprinting: Past, Present, Future** Biomaterials, 102 (2016), pp. 20-42 doi: 10.1016/j.biomaterials.2016.06.012

Hart et al. 2016 L. R. Hart, S. Li, C. Sturgess, R. Wildman, J.R. Jones, W. Hayes **3D Printing of Biocompatible Supramolecular Polymers and their Composites** ACS Appl. Mater. Interfaces**,** 8 (2016), pp. 3115-3122 doi: 10.1021/acsami.5b10471

He et al., 2016 Y. He, C.J. Tuck, E. Prina, S. Kilsby, S.D. Christie, S. Edmondson, R.J. Hague, F.R. Rose, R.D. Wildman **A new photocrosslinkable polycaprolactone-based ink for three-dimensional inkjet printing** J. Biomed. Mater. Res. Part B, 00B (2016) 000-000 doi: 10.1002/jbm.b.33699

Hoffman, 2002 A.S. Hoffman **Hydrogels for biomedical applications**, Adv. Drug Delivery Rev., 43 (2002), pp. 3-12 doi: 10.1016/S0169-409X(01)00239-3

Hsu et al., 2015 H-Y. Hsu, M.T. Harris, S. Toth, G. J. Simpson **Drop Printing of Pharmaceuticals: Effect of Molecular Weight on PEG Coated-Naproxen/PEG3350 Solid Dispersions** AIChE Journal, 61 (2015), pp. 4502-4508 doi: 10.1002/aic.14979

Içten et al., 2015 E. Içten, A. Giridhar, L.S. Taylor, Z.K. Nagy, G.V. Reklaitis **Dropwise additive manufacturing of pharmaceutical products for melt-based dosage forms** J. Pharm. Sci., 104 (2015), pp. 1641-1649 doi: 10.1002/jps.24367

Khaled et al., 2015 S.A. Khaled, J.C. Burley, M.R. Alexander, J. Yang, C.J. Roberts **3D printing of five-in-one dose combination polypill with defined immediate and sustained release** J. Control. Release, 217 (2015), pp.308-314. doi: 10.1016/j.jconrel.2015.09.028

Khaled et al., 2015 S.A. Khaled, J.C. Burley, M.R. Alexander, J. Yang, C.J. Roberts **3D printing of tablets containing multiple drugs with defined release profiles** Int. J. Pharm., 494 (2015), pp.643-650. doi: 10.1016/j.jconrel.2015.09.028

Korsmeyer et al., 1983 R.W. Korsmeyer, R. Gurny, E. Doelker, P. Buri, N.A. Peppas **Mechanisms of solute release from porous hydrophilic polymers** Int. J. Pharm., 15 (1983), pp. 25-35 doi: 10.1016/0378-5173(83)90064-9

Lee et al., 2012 B.K. Lee, Y.H. Yun, J.S. Choi, Y.C. Choi, J.D. Kim, Y.W. Cho **Fabrication of drug-loaded polymer microparticles with arbitrary geometries using a piezoelectric inkjet printing system** Int. J. Pharm., 427 (2012), pp. 305-310 doi: 10.1016/j.ijpharm.2012.02.011

Lin-Vien et al., 1991 D. Lin-Vien, N.B. Colthup, W.G. Fateley, J.G. Grasselli, The Handbook of Infrared and Raman Characteristic Frequencies of Organic Molecules, Academic Press, San Diego, 1991 doi: 10.1016/B978-0-08-057116-4.50016-X

Martin and Hutchings, 2012 G.D Martin, I.M. Hutchings **Fundamentals of Inkjet Technology**, in: I.M. Hutchings, G.D Martin (Eds.), Inkjet Technology for Digital Fabrication, Wiley-VCH, Weinheim, 2012, pp. 21-44 doi:10.1002/9781118452943.ch2

Maximilien, 2009 J. S. Maximilien **Polyethylene Oxide**, in: R. C. Rowe, P.J. Sheskey, M. E. Quinn (Eds.), Handbook of Pharmaceutical Excipients, Sixth ed., Pharmaceutical Press, London, 2009, pp. 522-524

McGilvray, 2010 K.L. McGilvray, *Doctoral Thesis*, University of Ottawa (Canada), 2010

Norman et al., 2017 J. Norman, R.D. Madurawe, C.M.V. Moore, M. A. Khan, A. Khairuzzaman **A new chapter in pharmaceutical manufacturing: 3D-printed drug products** Adv. Drug Deliv. Rev., 108 (2017), pp. 39-50 doi: 10.1016/j.addr.2016.03.001

O'Neil, 2012 B. O'Neil **Three-Dimensional Digital Fabrication,** in: I.M. Hutchings, G.D Martin (Eds.), Inkjet Technology for Digital Fabrication, Wiley-VCH, Weinheim, 2012, pp. 325-342 doi: 10.1002/9781118452943.ch14

Okwuosa et al., 2106 T.C. Okwuosa, D. Stefaniak, B. Arafat, A. Isreb, K.W. Wan, M.A. Alhnan **A Lower Temperature FDM 3D Printing for the Manufacture of Patient-Specific Immediate Release Tablets** Pharm. Res., 33(2016), pp. 2704-2712. doi: 10.1007/s11095-016-1995-0

Palo et al., 2015 M. Palo, R. Kolakovic, T. Laaksonen, A. Määttänen, N. Genina, J. Salonen, J. Peltonen, N. Sandler **Fabrication of drug-loaded edible carrier substrates from nanosuspensions by flexographic printing** Int. J. Pharm., 494 (2015), pp. 603-610 doi: 10.1016/j.ijpharm.2015.01.027

Palo et al., 2017 M. Palo, K. Kogermann, I. Laidmäe, A. Meos, M. Preis, J. Heinämäki, N. Sandler **Development of Oromucosal Dosage Forms by Combining Electrospinning and Inkjet Printing** Mol. Pharmaceutics, 14 (2017), pp. 808-820 doi: 10.1021/acs.molpharmaceut.6b01054

Pardeike et al., 2011 J. Pardeike, D.M. Strohmeier, N. Schrödl, C. Voura, M. Gruber, J.G. Khinast, A. Zimmer **Nanosuspensions as advanced printing ink for accurate dosing of poorly soluble drugs in personalized medicines** Int. J. Pharm., 420 (2011), pp. 93-100 doi: 10.1016/j.ijpharm.2011.08.033

Parmar et al., 2009 G. Parmar, S. Sharma, K. Singh, G. Bansal **Forced Degradation Study to Develop and Validate Stability-Indicating RP-LC for Quantification of Ropinirole Hydrochloride in Its Modified Release Tablets** Chroma., 69 (2009), pp.199-206. doi: 10.1365/s10337-008-0866-1

Raijada et al., 2013 Raijada, N. Genina, D. Fors, E. Wisaeus, J. Peltonen, J. Rantanen, N. Sandler **A step toward development of printable dosage forms for poorly soluble drugs** J. Pharm. Sci., 102 (2013), pp. 3694-3704 doi: 10.1002/jps.23678

Reddy et al., 2014 P.S. Reddy, A. M. Reddy, S. J. Reddy, S. Sait, K. Vyas **Impurity Profiling of the Ropinirole Extended Release Formulation, Identification and Characterization of Potential Degradant** J. Liq. Chromatogr. Relat. Technol., 37(2014), pp. 2490-2505. doi: 10.1080/10826076.2013.850720

Riger and Peppas, 1987 P.L. Ritger, N.A. Peppas **A simple equation for description of solute release I. Fickian and non-fickian release from non-swellable devices in the form of slabs, spheres, cylinders or discs** J. of Control. Release, 5 (1987), pp. 23-36 doi: 10.1016/0168-3659(87)90034-4

Rowe et al., 2000 C.W. Rowe, W.E. Katstra, R.D. Palazzolo, B. Giritlioglu, P. Teung, M.J. Cima **Multimechanism oral dosage forms fabricated by three dimensional printing** J. Control. Release, 66 (2000), pp. 11-17 doi: 10.1016/S0168-3659(99)00224-2

Sadia et al., 2016 M. Sadia, A. Sośnicka, B. Arafat, A. Isreb, W. Ahmed, A. Kelarakis, M.A. Alhnan **Adaptation of pharmaceutical excipients to FDM 3D printing for the fabrication of patient-tailored immediate release tablets** Int. J. Pharm., 513(2016), pp. 659-668 doi: 10.1016/j.ijpharm.2016.09.050

Sandler et al., 2011 N. Sandler, A. Määttänen, P. Ihalainen, L. Kronberg, A. Meierjohann, T. Viitala, J. Peltonen **Inkjet printing of drug substances and use of porous substrates-**

towards individualized dosing J. Pharm. Sci., 100 (2011), pp. 3386-3395 doi:10.1002/jps.22526

Saunders and Derby, 2014 R.E. Saunders, B. Derby **Inkjet printing biomaterials for tissue engineering: bioprinting** Int. Mater. Rev., 59 (2014), pp. 430-448 doi: 10.1179/1743280414Y.0000000040

Scoutaris et al., 2011 N. Scoutaris, M.A. Alexander, P. R. Gellert, C.J. Roberts **Inkjet printing as a novel medicine formulation technique** J. Control. Release, 156 (2011), pp. 179-185 doi: 10.1016/j.jconrel.2011.07.033

Soltman and Subramanian, 2008 D. Soltman, V. Subramanian **Inkjet-Printed Line Morphologies and Temperature Control of the Coffee Ring Effect** Langmuir, 24 (2008), pp. 2224-2231 doi: 10.1021/la7026847

USP, 2000 United States Pharmacopeia and National Formulary (USP 24- NF 19), The United States Pharmacopeial Convention, Rockville, MD, USA 2000

USP, 2014 United States Pharmacopeia and National Formulary (USP 37- NF 32), 1st Suppl., The United States Pharmacopeial Convention, Rockville, MD, USA 2014

Varan et al., 2017 C. Varan, H. Wickström, N. Sandler, Y. Aktaş, E. Bilensoy **Inkjet Printing of Antiviral PCL Nanoparticles and Anticancer Cyclodextrin Inclusion Complexes on Bioadhesive Film for Cervical Administration** Int. J. Pharm. (2017) https://doi.org/10.1016/j.ijpharm.2017.04.036

Vehse et al., 2014 M. Vehse, S. Petersen, K. Sternberg, K-P. Schmiz, H. Seiz **Drug Delivery From Poly(ethylene glycol) Diacrylate Scaffolds Produced by DLC Based Micro-Stereolithography** Macromol. Symp., 346 (2014), pp. 43-47 doi:10.1002/masy.201400060

Wang et al., 2016 J. Wang, A. Goyanes, S. Gaisford, A.W. Basit **Stereolithographic (SLA) 3D printing of oral modified-release dosage forms** Int. J. Pharm., 503 (2016), pp. 207-212 doi: 10.1016/j.ijpharm.2016.03.016

Williams et al., 2005 C.G. Williams, A. N. Malik, T.K. Kim, P.N. Manson, J.H. Elisseeff **Variable cytocompatibility of six cell lines with photoinitiators used for polymerizing hydrogels and cell encapsulation** Biomaterials, 25 (2005), pp. 1211-1218 doi:10.1016/j.biomaterials.2004.04.024

Xu et al., 2015 L. Xu, N. Sheybani, W. A. Yeudall, H.Yang **The effect of photoinitiators on intracellular AKT signalling pathway in tissue engineering application** Biomater. Sci., 3 (2015), pp. 250-255 doi: 10.1039/C4BM00245H

Yeates et al., 2012 S. G. Yeates, D. Xu, M-B. Madec, D. Caras-Quintero, K.A. Alamry, A. Malandraki, V. Sanchez-Romaguera, **Fluids for Inkjet Printing**, in: I.M. Hutchings, G.D Martin (Eds.), Inkjet Technology for Digital Fabrication, Wiley-VCH, Weinheim, 2012, pp. 87-112 10.1002/9781118452943.ch4

Zhu et al., 2013 Q. Zhu, S.J. Toth, G.J. Simpson, H-Y. Hsu, L.S. Taylor, M.T. Harris **Crystallization and dissolution behavior of naproxen/polyethylene glycol solid dispersions** J. Phys. Chem. B., 117 (2013), pp. 1494-1500 doi: 10.1021/jp3106716

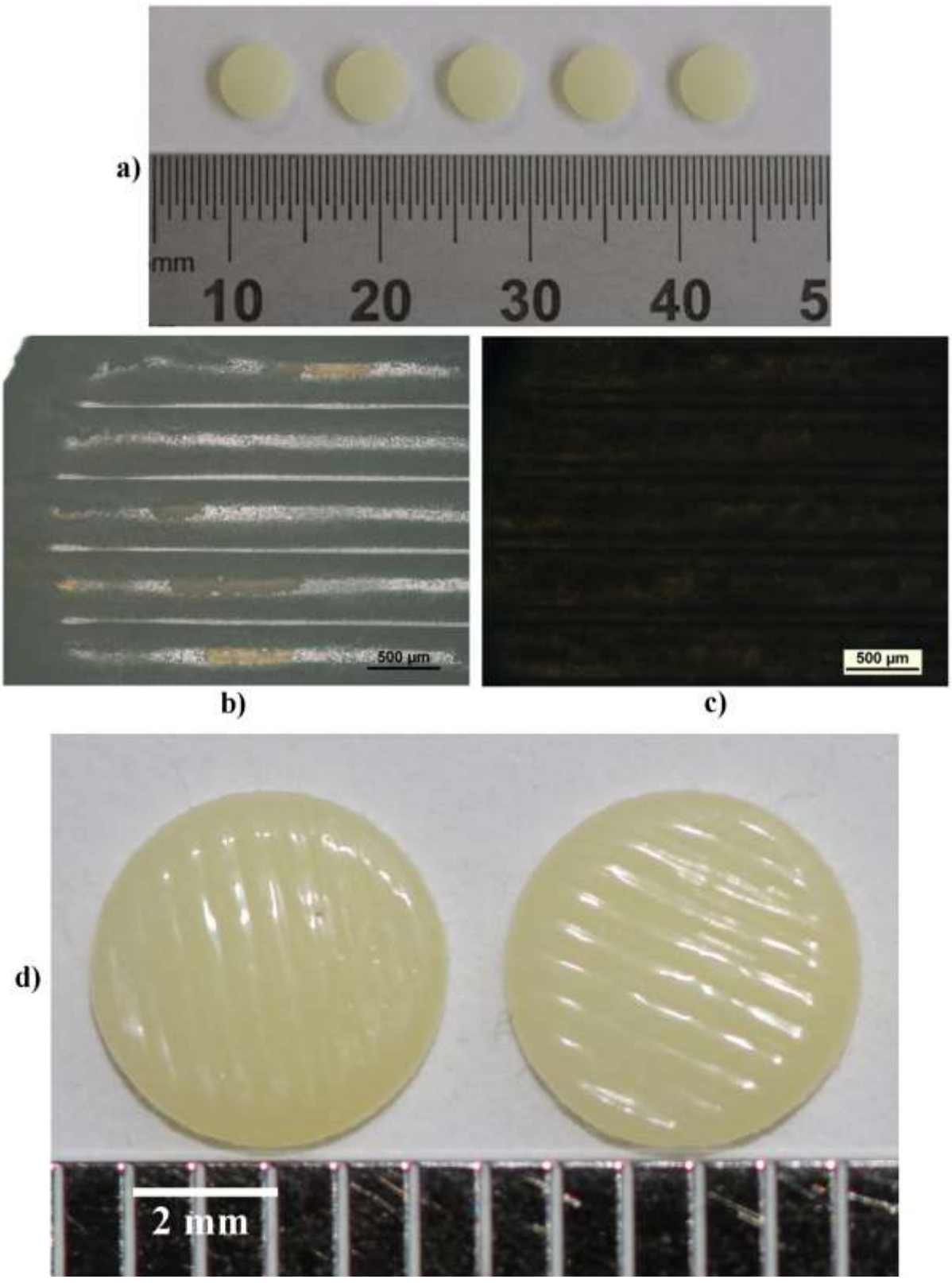

Fig. 1.

Images of ropinirole HCl printed tablets. **a, d)** Image of tablets with 115 layers +10 non-jetting post curing print passes. **b)** Reflection (5x) and **c)** transmission cross polarized (5x) optical

microscopy images of the top surfaces of the API loaded tablets, respectively. Microscope used as a Nikon Eclipse LV100ND Polarizing microscope (Nikon U.K. Ltd., Surry, UK).

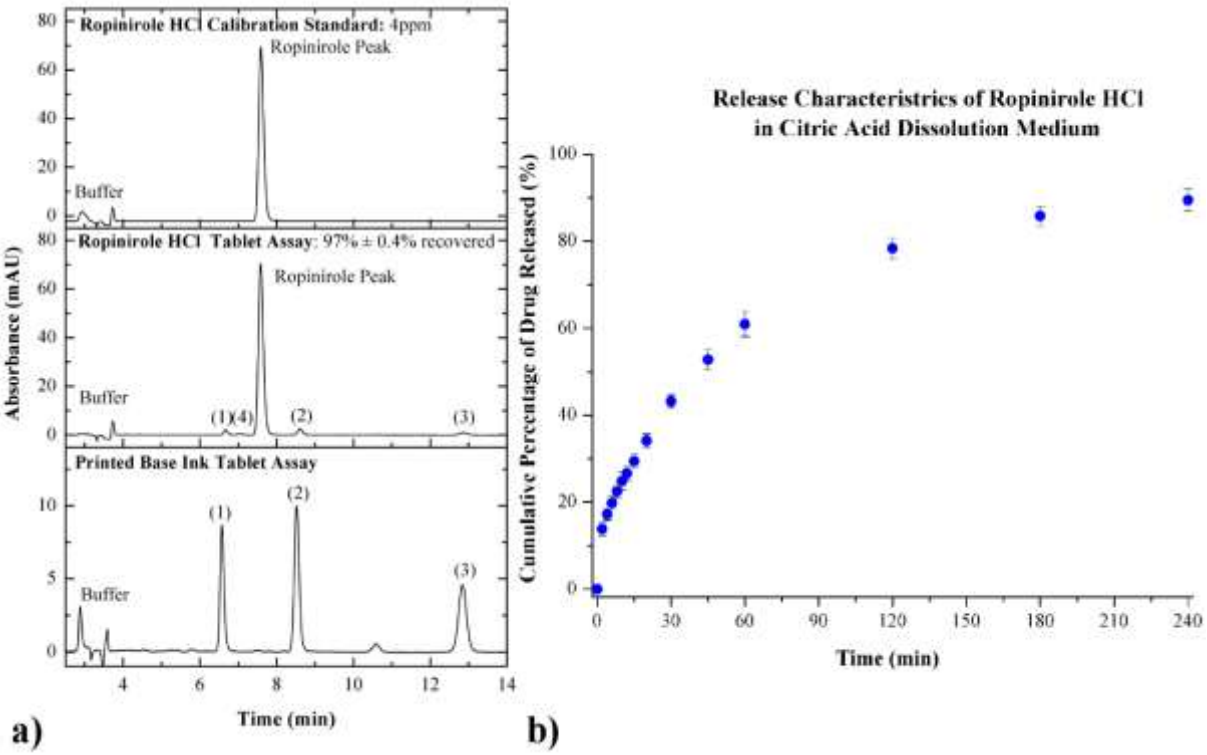

Fig. 2.

Quantification of drug release from the printed tablets. **a)** HPLC chromatogram of the 4ppm ropinirole HCl standard (top), API tablet assay, and printed base ink tablet assay (bottom). **b)** USP II dissolution profile ropinirole HCl release from the tablets in citric acid dissolution medium (pH= 4.00). Standard deviation is shown as error bars (*n=10*).

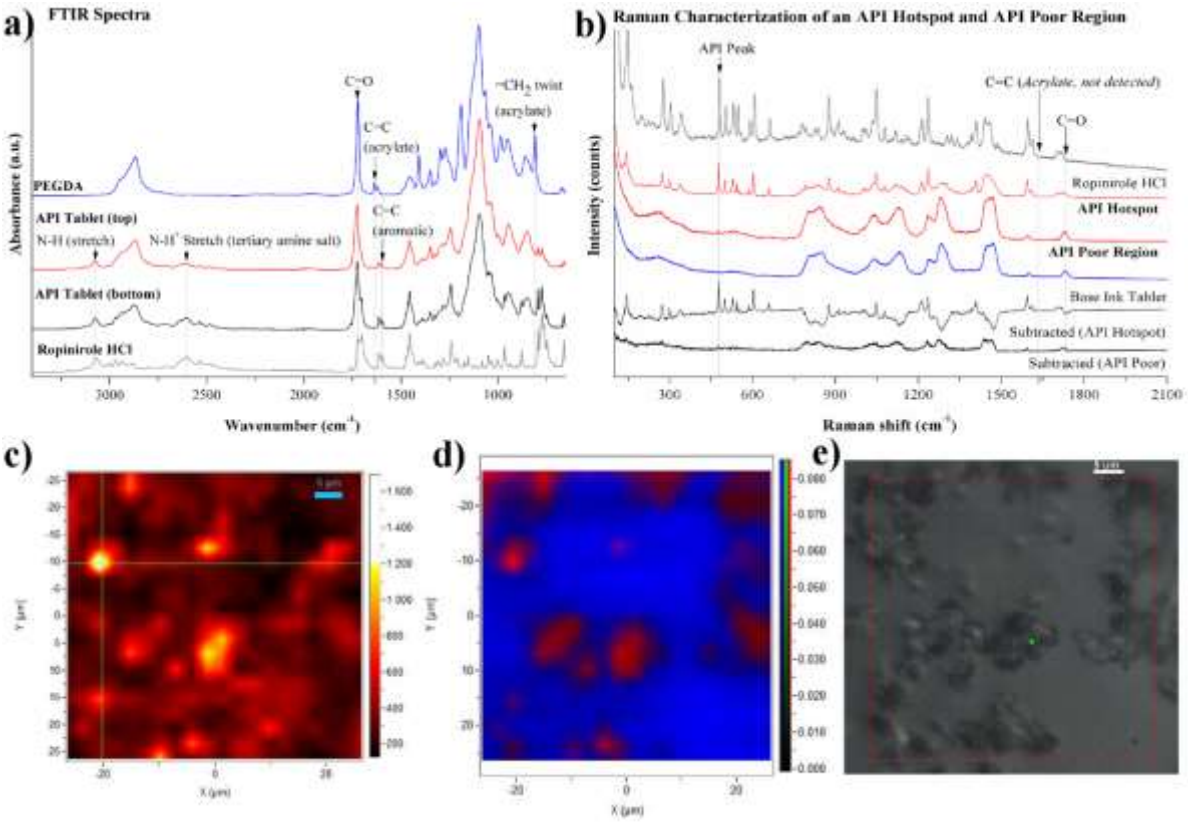

Fig. 3.

a) FTIR of the formulation components and API tablet surfaces. **b)** Single point Raman spectra of the pure drug (grey), printed base ink (blue), top tablet surface (red) and subtracted spectra (black). Both a drug rich and drug poor spectra are shown for the tablet. Subtracted spectra were calculated as the difference between the tablet spectra and the printed base ink. **c)** Raman intensity mapping of the API peak over a 50 μm x 50 μm area. **d)** Classical least squares fit (CLS) of ropinirole HCl (red) and the base ink (blue) of the tablet. Both intensity mapping and CLS fit indicate that the dosage form is a solid dispersion with drug rich and poor regions. **e)** A 50x optical microscopy image of the mapped area, as well as the overlaid map coordinates (red) and laser location (green). Laser: IR 784 nm, step 2.5 μm, 400 pts.

Table 1.

Physical Properties of API loaded Tablets. Mass, diameter, and print height of two batches of twenty five tablets. Diameter and height were measured with an electronic caliper (Products Engineering Corp., USA).

Batch no.	Mass [mg][a)]	Diameter [mm][b)]	Height [mm][c)]
1	14.31 +/- 0.04[d)]	5.03 +/- 0.01	0.72 +/- 0.02
2	14.17 +/- 0.03	5.02 +/- 0.02	0.72 +/- 0.01

[a)](n= 25 tablets); [b)](n= 10 tablets); [c)](n= 10 tablets); [d)] (values reported as mean +/- standard deviation)

Table 2.

Degree of swelling and leaching in the API and base ink tablets at 37ºC. Tablets were leached for nine days in 10mL deionized water. Percent extractable = 100 x (Initial Dry Mass –Final Dry Mass)/ Initial Dry Mass. Degree of swelling = 100 x (Swelled Hydrogel Mass –Final Dry Mass)/ Final Dry Mass.

API tablets

Tablet no.	Initial Dry Mass [mg]	Final Dry Mass [mg]	Swollen Hydrogel Mass [mg]	Percent extractable [%]	Degree of Swelling [%]
2	14.16	13.30	20.01	6.073	50.45
23	14.08	13.49	19.90	4.190	47.52
6	14.03	13.45	19.77	4.134	46.99
12	14.09	13.36	19.76	5.181	47.90
14	14.12	13.41	19.71	5.028	46.98
Avg.	14.10	13.40	19.83	4.921	47.97
S.D.	0.05	0.07	0.12	0.800	1.44

Base ink tablets

Tablet no.	Initial Dry Mass [mg]	Final Dry Mass [mg]	Swollen Hydrogel Mass [mg]	Percent extractable [%]	Degree of Swelling [%]
17	14.98	14.45	20.89	3.538	44.57
10	14.75	14.36	20.62	2.644	43.59
6	14.8	14.36	20.95	2.973	45.89
19	14.76	14.39	20.78	2.507	44.41

11	14.76	14.41	20.85	2.371	44.69
15	14.67	14.30	20.74	2.522	45.03
13	14.76	14.51	20.79	1.694	43.28
Avg.	14.79	14.39	20.79	2.696	44.48
S.D.	0.08	0.07	0.10	0.592	0.90